Bull. Disas. Prev. Res. Inst., Kyoto Univ., Vol. 41, Part 1, No. 354, March, 1991 

# Strain Variations of the Yamasaki Fault Zone, Southwest Japan, Derived from Extensometer Observations

## Part 1 — On the Long-term Strain Variations —

By Kunihiko WATANABE

(Manuscript received on February 5, 1991)

**Abstract**

The Yamasaki fault is one of the active, left-lateral, strike-slip faults in Southwest Japan. Various kinds of observations are carried out at the Yamasaki Fault Observation Station, as part of the national project for earthquake prediction in Japan. The most fundamental observation at this station has been made by twelve component extensometers which are set in two observation tunnels mutually perpendicular and crossing the Yamasaki fault. Long-term strain variations of the fault zone were analyzed in this study. Zigzag secular variations with intervals of a few years were observed by most components. These strain variations are approximately $5\times10^{-6}$ strain and normal to the fault zone, so that it is interpreted as the thickness change of the fault zone. Moreover, it was clarified that those turning points of the alternations correspond to the changes in seismic activity around the Yamasaki fault.

## 1. Introduction

In the latter half of the 1960's, a linear distribution of epicenters of microearthquakes along the Yamasaki fault in Hyogo Prefecture, Southwest Japan was revealed by the observations of the Tottori Microearthquake Observatory, Disater Prevention Research Institute, Kyoto University.[1),2)] In nearly the same period, topographic investigations showed that the Yamasaki fault is an active fault of left-lateral, strike-slip type.[3)] These two investigations strongly suggested that earthquake occurrence is closely related to active fault movement, and that various geophysical observations concerning active faults are necessary to clarify general earthquake mechanism as to advance earthquake prediction researches specifically in this region.[4)]

For these purposes, various kinds of observations including crustal deformation, earthquake activity, geomagnetism and geoelectricity, underground water, radioactivity and others were commenced in 1975.[5)] This observation project was adopted in 1978 as a Test-Field Project for earthquake prediction in Japan.[6),7)] This project aimed at the prediction of moderate and small earthquakes considered to occur rather frequently.

The observation by extensometers[8),9)] installed in an observation vault crossing the Yamasaki fault is most fundamental to understand the fault movement and its relation to earthquake occurrence around the fault. It is necessary to understand characteristics of

strain behaviors observed in the vault in order to detect any strain changes related to earthquakes.

In this article, investigations on characteristics of daily, annual and secular strain changes are preserved.

## 2. The Yamasaki fault and the extensometer observation system

### 2. 1 The Yamasaki fault

The Yamasaki fault is one of the quaternary left-lateral active faults situated in southwest Japan[10] with a NWW-SEE strike and a length of about 80 kilometers. As shown in **Fig. 1,** the Yamasaki fault actually consists of five faults; Ohara, Hijima, Yasutomi, Kuresaka-toge, and Miki faults, in order from NWW to SEE. The extent of left-lateral dislocations along the fault ranges from some tens to several hundreds of meters.[11)~13)] The Yamasaki Fault Observation Station is located on the Yasutomi fault. Near the observation station, the thickness of the Yasutomi fault and the fault dislocation are about 100 and 200 meters, respectively. The Chugoku Expressway lies just upon the Yasutomi fault. The Yasutomi Observation Vault, which crosses the main fractured zones of the Yasutomi fault, was constructed under the Chugoku Expressway (**Fig. 2**).

According to the Geological Survey of Japan (1981)[14], mesozoic rhyolite, paleozoic slate and sandstone are distributed in the Yasutomi fault region. These rhyolite and slate

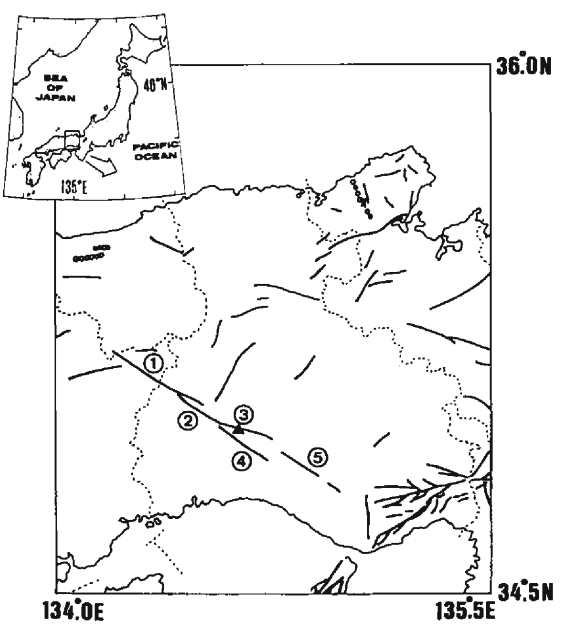


Fig. 1. Distribution of active faults in the western Kinki district.[9] The Yamasaki fault consists of five major active faults, namely, (1) Ohara, (2) Hijima, (3) Yasutomi, (4) Kuresaka-toge and (5) Miki faults, respectively. The solid triangle denotes the Yamasaki Fault Observation Station.

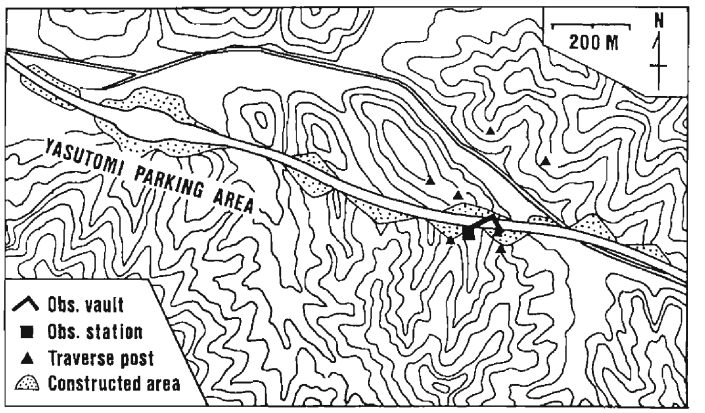


Fig. 2. Topography around the Yamasaki Fault Observation Station (■). The Chugoku Expressway lies east–west near the station and the Yasutomi Observation Vault (L –shaped) has been situated just under the expressway. Solid triangles denote the traverse posts of the Yasutomi–Usuzuku Baseline Network for geodetic measurements.

were identified in the core samples obtained by a boring near the station.[15] The "Harima earthquake" of M7 in 868 probably occurred by the dislocations along the Yasutomi fault.[16] According to the Japan Meteorological Agency[17], moderate earthquakes with magnitudes greater than or equal to 5.0 have occurred along the Yamasaki

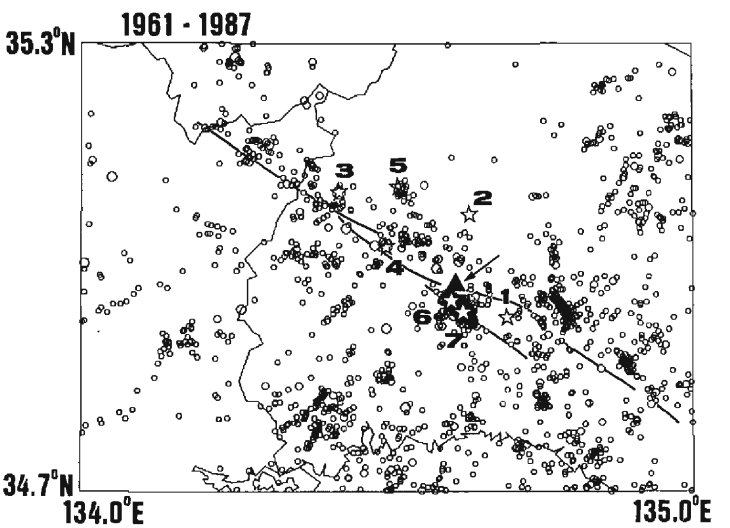


Fig. 3a. Distribution of microearthquakes of M≧1.6 and H≦40km obtained by the Tottori Microearthquake Observatory[36], from 1961 to 1987. Asterisks with numerals denote the epicenters of M≧5 determined by J. M. A., from 1926 to 1987. The solid lines and the solid triangle with an arrow show the Yamasaki fault and the Yamasaki Fault Observation Station, respectively.

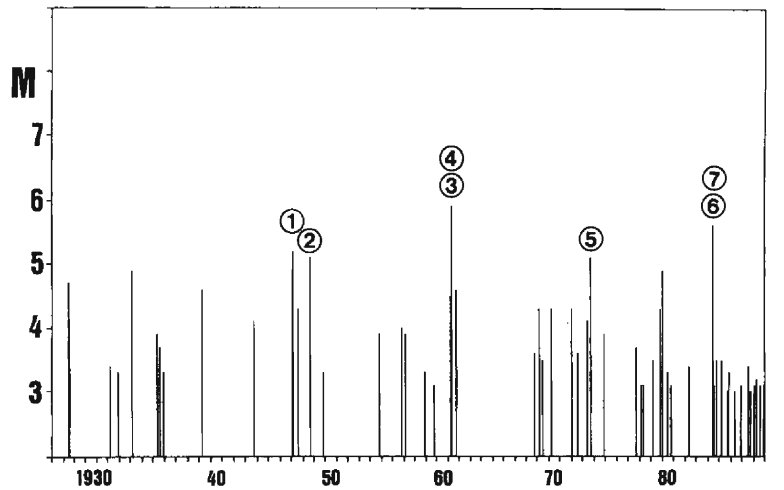


Fig. 3b. Time series of earthquakes of M≧3 by J. M. A.. Numerals correspond to the earthquakes of M≧5 illustrated in **Fig. 3a.** Periodical activities with time intervals of 11～13 years can be recognized.

fault periodically with 11–13 years' intervals over the past fifty years. Therefore, the Yamasaki fault is highly active to be worth investigation (**Figs. 3a, b**).

### 2. 2 Observation station and data processing

In **Fig. 2,** the topography near the Yamasaki Fault Observation Station and the Yasutomi Observation Vault are illustrated. The Yasutomi fault contains some fractured zones which run almost parallel to the fault strike. The vault consists of two tunnels which are perpendicular to each other and crossing the main fractured zone at about 45 degrees.

In **Fig. 4,** the spatial relation between the Yasutomi Observation Vault and the Chugoku Expressway is illustrated. The Chugoku Expressway inclines about 2.6% westward near the observation vault.[18] The tunnel in the direction of N34°W is named A–tunnel and that of N56°E is B–tunnel. The overburden depths are about eight meters at the entrance of A–tunnel and six meters at the southwestern end of B–tunnel, respectively. As the corner of the vault is located under the mountainous part north of the expressway, the overburden depth is much deeper there.

The distribution of the displacement sensors of extensometers is also shown in **Fig. 4,** and the locations of major fractured zones are illustrated by shadows. The fractured zones between sensors No. 2 and No. 3 and between No. 10 and No. 11 are the portions of the main fractured zone which were confirmed by the observations on the ground surface.[19] The rod along A–tunnel is called A–rod, and that along B–tunnel is B–rod. In order to detect characteristic behaviors of the fractured zones, six displacement sensors (No. 1 to 6) are distributed on A–rod, and five sensors (No. 8 to 12) are on B–rod. The fixed–ends of these two rods are situated at the corner of the vault. In this article, we call the strain between the fixed–end and i–th sensor "fixed–end strain of component

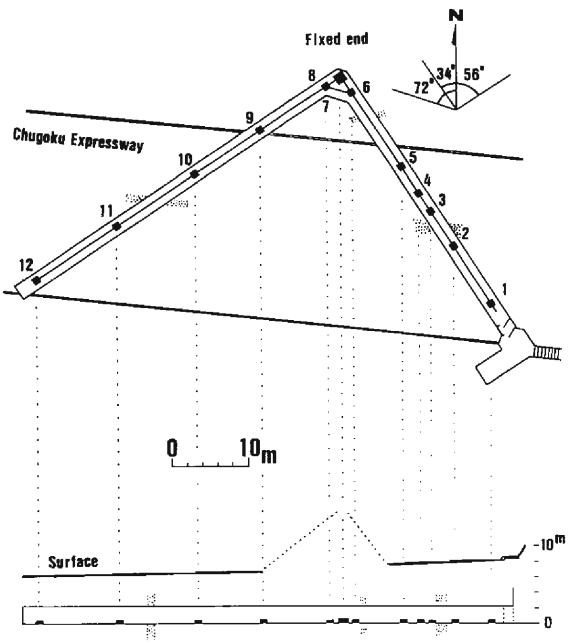


Fig. 4. Spatial relation between the observation vault and the Chugoku Expressway. Numerals denote the displacement sensors of the extensometers. Some fractured zones which were confirmed by geological survey are indicated by shadows. The lower figure shows the vertical plane of the site. The middle part of the lower figure is located under the northern mountainous area.

0–i". Thus, it is possible to calculate strains between any two sensors from the difference of displacements of the two sensors. We call the strain between i–th and j–th sensors "partial strain of component i–j". The third extensometer has been located at the corner of the vault, whose direction is N72°W, almost parallel to the Yasutomi fault. The fixed–end of this extensometer is on the same base that sensor No. 6, and the displacement sensor is on the same base that No. 8. This is named the strain component 6–7.

The extensometer rods consist of super–invar pipes. All of the displacement sensors and the ends of the rods are fixed to concrete piers which are directily attached on the bed rock. A differential transformer is used for the displacement sensor. The coil part of it is attached to the extensometer rod and the core part is settled on the basement rock by using a micrometer with a reduction gear. As these two parts do not contact each other, no frictional strain is accumulated between the rod and the basement rock. Sensitivity of each displacement sensor is annually calibrated by moving the micrometer at a constant rate. The temporal fluctuation of magnification coefficients is about 2% throughout all displacement sensors. The normality of rods is also certified by adding external force to the ends of the rods and then removing it. The extensometer observations in the Yasutomi Observation Vault started in November 1975.[8] Except for the first month of observations, there were no apparent systematic drifting strain variations which were considered to be caused by deformation of instruments. Judging from the records,

Table 1. Lengths and directions of extensometers

| sensor No. | aistance from the fixed end | direction of the rod |
|---|---|---|
| 1 | 35.78$^{m}$ | N34°W |
| 2 | 26.86 | 〃 |
| 3 | 21.49 | 〃 |
| 4 | 18.60 | 〃 |
| 5 | 14.55 | 〃 |
| 6 | 3.02 | 〃 |
| 7 | 3.82 | N72°W |
| 8 | 2.40 | N56° E |
| 9 | 12.76 | 〃 |
| 10 | 22.76 | 〃 |
| 11 | 34.83 | 〃 |
| 12 | 47.89 | 〃 |

we consider there is no significant drift of the extensometers.

As the Chugoku Expressway lies just six to eight meters above the observation vault, the high frequency traffic noises overlaps the natural strain variations. In order to reduce these traffic noises, low-pass filters with cut-off periods of one minute have been applied. The output data are sent to the Disaster Prevention Research Institute of Kyoto University in Uji by a public telephone line. Evaluating the whole process of the system, the absolute time accuracy of those extensometer data is within two minutes and the detectability is about $10^{-9}$ strain. **Table 1** shows the directions of the rods and distances between each sensor and the fixed-end.

In the following analyses, hourly strain data are used for daily variation analyses. For secular analyses daily data are used, which are momentary data at the moment of 00h00m every day. Artificial disturbances and lack of data have been compensated for, and continuous data sets have been used for analyses. More details on the Yamasaki Observation Station and the observation system are described by Oike et al (1981).[20]

## 3. Characteristic behaviors of the strain variations at the Yasutomi Observation Vault

It is supposed that the observed strain variations are influenced by many kinds of factors. As for the Yasutomi Observation Vault, the observed strain variations are complicated because of the fractured zones of the fault and shallowness of the vault. It is important, however, to understand the features of observational data of extensometers in order to find out relations between earthquake occurrence and the characteristic behaviors of the fault. In this section, we will try to elucidate the characteristics of the fault by analyzing the daily, annual and long-term strain variations.

### 3. 1 Daily strain variations

Typical daily strain variations both in summer and in winter are illustrated in **Figs. 5a** and **b** with air temperature variations observed at the Yamasaki Fault Observation Station. Fourier's spectral analyses, which have been carried out on hourly data for one or

three months, indicate that the amplitudes of those daily strain variations are almost the same as or greater than the amplitudes of $M_2$ component of earth tides. Theoretically, the amplitudes of daily tidal strains are smaller than those of $M_2$ component at this latitude. Therefore, the observed daily strain variations with larger amplitudes than $M_2$ component are not $O_1$, $K_1$ or any other diurnal component of earth tides.[21]

On the other hand, some rainy days are included in the figures. The amplitudes of the air temperature during those rainy days were small, and the amplitudes of daily strain variations were also small. Therefore, these daily strain variations are considered to be originated by daily temperature variations of the ground surface. The amplitudes of those daily strain variations were generally greater in B-tunnel than in A-tunnel, and slso greater in summer than in winter.

In general, two kinds of mechanisms can be considered by which the temperature variations affect the strain variations. One is the effect which can be explained mainly by thermoelasticity and the other is that by heat conduction.[22), 23)]

We obtained the phase delays of those daily strain variations from the air temperature by using a cross-correlation method (**Fig. 5c**). As can be seen in **Figs. 5a, b** and **c,** the strain variations in A-tunnel, with the exception of component 0-6, showed negative correlation to the air temperature variations with phase delays of two to three hours. On the contrary, all components in B-tunnel, the third component of 6-7 and component 0-6 showed positive correlation to the temperature with three to four hours delay. Thus, the displacement sensors are divisible into two groups, a group of negative correlation, No. 1-No. 5, and the other group of positive correlation, No. 6-No. 12. The mechanism which divides the daily strain variations spatially into two groups can not be explained by the model in which heat conducts downwards from the ground surface and creates the thermal deformations of the basement rock where the extensometers are settled. Accordingly, the heat conduction model should be rejected. On the ground surface near the observation vault, an artificial topography extending east-west has been made by the construction of the Chugoku Expressway. Therefore, the rather short wave length of topography predominates in the N-S direction near the Yasutomi Observation Vault. It is supposed that the surface temperature variations originate a modified deformation by this topography and that this surface deformation transfers into the ground as daily thermoelastic strain wave. In **Fig. 5c,** phase delays of about two to four hours can be seen in both spatially separated groups. If a visco-elastic layer exists between the road surface and the observation vault, the above mentioned phase delays might be explained.

The amplitudes of daily strain variations range from $2\times10^{-8}$ to $5\times10^{-7}$ in summer, which are comparable to those of earth tides. On the other hand, in winter, these amplitudes seem to range from $10^{-8}$ to $5\times10^{-8}$ strain. These seasonal differences can be explained by the fact that the absolute temperature level in summer is higher than in winter, causing surface deformations of the expressway to be larger in summer, in spite of the same amplitude of air temperature variation.

### 3. 2 Annual strain variations

The strain variations for twelve years are plotted in **Figs. 6a** and **b** by using daily

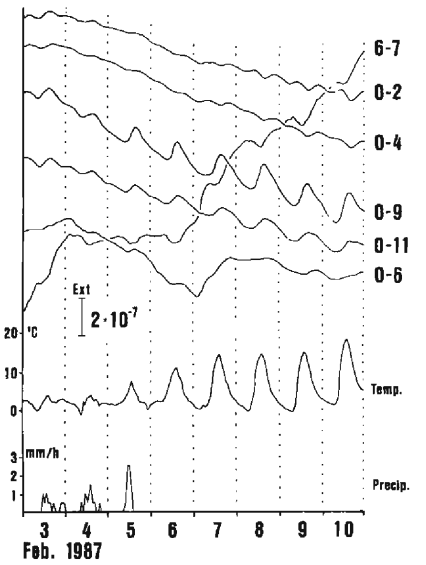


Fig. 5a

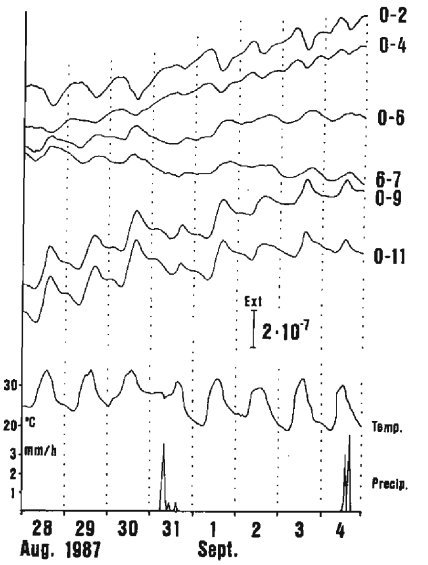


Fig. 5b

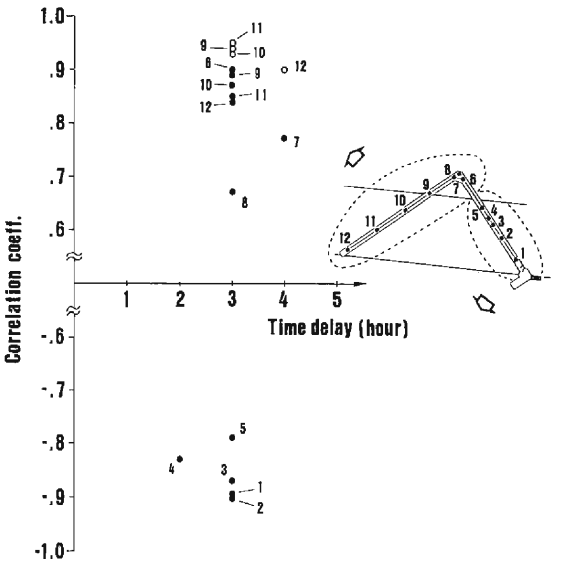


Fig. 5c

Fig. 5a. Daily strain variations of representative components in winter caused by the daily variations of surface air temperature and precipitation.

Fig. 5b. Daily strain variations of representative components in summer.

Fig. 5c. Cross correlation coefficients and time delays between the surface air temperature and each strain ccomponent. Each numeral denotes the fixed-end strain component, for example, "1" means the fixed-end strain component 0-1. Strain components are separated into two groups spatially (right hand side in the figure). Solid circles mean the results in summer and open ones, in winter.

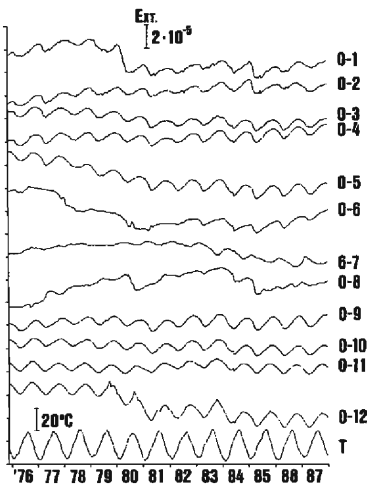


Fig. 6a

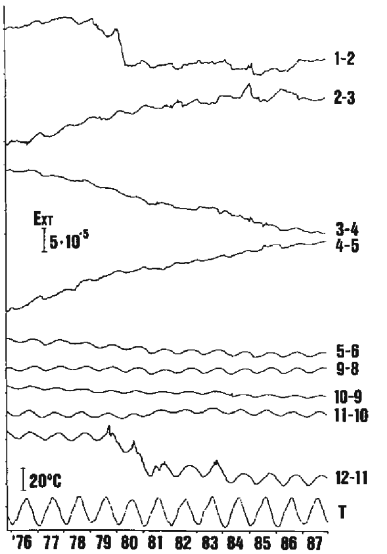


Fig. 6b

Fig. 6a. Variations of fixed-end strains. "*T*" denotes the surface air temperature variations obtained by using the daily maximum and minimum values at Himeji Weather Station.

Fig. 6b. Varitions of partial strains.

values. The annual variations are remarkable on all components. In general, meteorological phenomena, for example, ground surface temperature and precipitation, are considered to be the main factors which cause annual strain variations.[24] Since the Yasutomi Observation Vault is shallow, it can be anticipated that surface temperature variations considerably affect the strain variations. Precipitation also shows annual variation. However, the peak and trough of its annual variation change year by year and do not closely relate to the annual strain variations. Therefore, we do not consider annual variation in precipitation to affect the annual strain variations to any significant degree.

Nakano (1963)[22], Yoshioka and Nakano (1974)[23] discussed the ground strain caused by the annual variation in surface temperature. Tanaka (1972)[25] analyzed data observed at many crustal movement observatories. According to their results, the effects of thermal conductivity are greater than those of thermoelastic strain in the case of shallow vaults less than some tens of meters. Depth-dependent difference of both kinds of effects results from the difference of the periods between daily and annual variations of surface temperature. As the overburden depth of the Yasutomi Observation Vault ranges from six to eight meters, it is supposed that the effects of thermal conductivity are greater than those of thermoelasticity in the case of annual strain variations.

In order to investigate the effects of annual temperature variations, we used the air temperature data recorded at Himeji Weather Station[26], which is located about twenty kilometers from the Yamasaki Fault Observation Station. Because the air temperature

observations at the Yamasaki Fault Observation Station have not been continued long enough to analyze long-term phenomena, we compared our temperature data with those at Himeji Weather Station. Spatial differences in annual variations between the Yamasaki Fault Observation Station and Himeji Weather Station can be disregarded concerning such long-term analyses.

The observed amplitudes of annual variations range from $2\times10^{-6}$ to $7\times10^{-6}$ strain, which are one to three orders of magnitudes greater than those of the daily variations mentioned in **3. 1.** All components show positive correlation to the air temperature variation, differing from the case of daily variations. The main feature is that the amplitudes and phases slightly and systematically differ from component to component.

Some amount of phase delays of strains from the temperature are often recognized. Berger (1975)[27] and Ben-Zion (1986)[28] conjectured those phase delays from the standpoint of thermoelaticity by assuming a non-elastic thin layer beneath the ground surface. The ground surface just above the vault corresponds to the expressway in the most part and can be assumed to be flat in the present case. Therefore, the Yasutomi Observation Vault is the ideal place to show whether the systematic phase delays may be explained by the differences of overburden depths or not.

At first, we calculated Fourier's spectra of the air temperature variations at Himeji for the daily data from 1976 to 1987 and those of each fixed-end strain component separately. We obtained the phase differences between the air temperature and each fixed -end strain component, regarding the spectra of one year period. In **Table 2,** the results are shown in days.

There can be seen a tendency in **Table 2** that deeper overburden depth generates greater phase delay in the annual strain variation. Therefore, the mechanism of the

Table 2. Phase angles of annual variations in days. Numerls in the third column mean the phase delays of each fixed-end strain component from the temperature, expressed in days. The last column shows the depths obtained by using the phase delays in **Fig. 8.**

| strain component | minimum appearance | phase delay behind the temperature in days | calculated overburden depth in meters |
|---|---|---|---|
| Himeji temperature | 29.3 days (Jan. 29th) | | |
| 0 - 1 | | 152.5 days | 8.13 m |
| 0 - 2 | | 138.4 | 7.45 |
| 0 - 3 | | 119.4 | 6.43 |
| 0 - 4 | | 120.2 | 6.52 |
| 0 - 5 | | 115.5 | 6.31 |
| 0 - 6 | | 113.4 | 6.34 |
| 6 - 7 | | ( 238.1 ) | ( 13.48 ) |
| 0 - 8 | | ( 194.1 ) | ( 10.95 ) |
| 0 - 9 | | 113.8 | 6.61 |
| 0 - 10 | | 102.5 | 6.12 |
| 0 - 11 | | 77.5 | 4.91 |
| 0 - 12 | | 76.8 | 5.11 |

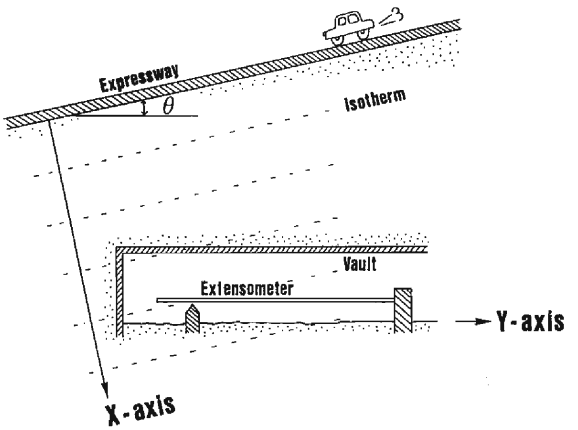


Fig. 7. Heat conduction model from the expressway surface into the ground.

annual variations is supposed to be mostly the thermal deformation caused by heat conducted from the ground surface. The gradual variations of phase delays in the annual variations cannot be explained by thermoelastic strain mechanism. The deviation of components 6–7 and 0–8 from the general tendency may be explained by the fact that the sensors of these two components are located under the northern mountainous region. Here, we assume a one-dimensional thermal conductivity model as shown in **Fig. 7**[29] in order to examine the heat conductivity mechanism at the Yasutomi Observation Vault. The effects of the cavity of the vault can be ignored in the following estimation, because of the low specific heat and low thermal conductivity coefficient of air.

In the figure, it is assumed that the observation vault is horizontal and the expressway surface is flat and inclines toward west at an angle $\theta$. The $X$-axis is taken perpendicular to the expressway surface, and the $Y$-axis is taken in the direction of the extensometer rod. Then, we can express,

$$y \cdot \sin\theta = x. \tag{1}$$

As the heat conducts only in the $X$-axis direction, the ground temperature, $T(t, x)$, makes isotherms parallel to the expressway surface. Since the vault and isotherms make an angle of $\theta$, the temperature of the vault differs in the horizontal direction.

The differential equation for one dimensional thermal conductivity is

$$\frac{\partial T}{\partial t} = \frac{K}{C\rho} \cdot \frac{\partial^2 T}{\partial x^2}, \tag{2}$$

where $T$ is the temperature and $x$ is the distance. $K$, $C$ and $\rho$ are thermal conductivity, specific heat and density, respectively. If the temperature on the ground surface ($x=0$) is uniform and only varies sinusoidally with a period of one year, we can write the temperature on the surface as,

$$T(t,\ 0)=T_0\cdot\cos(\omega t+\delta_0), \tag{3}$$

where $T_0$, $\omega$ and $\delta_0$ are the amplitude at the surface, angular frequency and initial phase, respectively. Then, we can obtain the temperature at the point $P(t,\ x)$ as,

$$T(t,\ x)=T_0\exp\left(-\sqrt{\frac{\omega}{2a}}x\right)\cos\left(\omega t-\sqrt{\frac{\omega}{2a}}x+\delta_0\right), \tag{4}$$

where $a=K/C\rho$ denotes thermal diffusivity. According to equation (4), the amplitude decreases exp $(-\sqrt{\omega/2a}\cdot x)$ times that on the ground surface and the phases are delayed $\sqrt{\omega/2a}\cdot x$ from that on the ground surface.

The temperature change from $t=t_1$ to $t=t_2$ at point $P(t,\ x)$ is

$$\Delta T=\int_{t_1}^{t_2}\frac{\partial T(t,\ x)}{\partial t}\,dt. \tag{5}$$

Then the strain change from $t=t_1$ to $t=t_2$, $\Delta\varepsilon$, can be obtained by

$$\Delta\varepsilon=\frac{1}{L}\int_0^L(\Delta T\cdot\beta)\,dy, \tag{6}$$

where $\beta$ is the linear coefficient for thermal expansion and $L$ is the length of the extensometer. Substituting $\Delta T$ of equation (5) into equation (6), we can get the annual strain variations. Since the theoretical strain amplitudes decrease exponentially to the depth as seen in equation (4) and the depth dependence of amplitude is small at the level of this vault, comparison of small change of the observed amplitude to theoretical one will introduce a large error. On the contrary, the phase delays vary in proportion to the depth. Accordingly, we try to calculate the overburden depths by using the phase delays.

We referred to the physical constants of granite (Rikanenpyo; 1989)[30] and assumed the values of parameters as $K=8\times10^{-3}$cal/cm • sec • deg, $C=0.3$cal/gr • deg and $\rho=2.5$gr /cm$^3$. In this case, the thermal diffusivity $a$, becomes $a=1.07\times10^{-4}$cm$^2$/sec. The practical calculations of the overburden depths corresponding to each fixed-end strain component were carried out by some iterative method. The results obtained are shown in **Fig. 8.** A chain line denotes the real road surface which inclines westward at a ratio of 2.6%.[18] The solid line shows the calculated road surface inclining at a ratio of 4.0% without using components 6–7 and 0–8. Although absolute depths differ by 0.5~1.5 meters from true values, the calculated results approximately coincide with the true depths of the vault. It is concluded that the observed annual strain variations can be explained by the in-situ deformation due to the thermal conductivity from the surface. The scattering of each point in **Fig. 8** might be caused by the local differences of the physical parameters.

The annual strain variations can be removed by using the air temperature data.

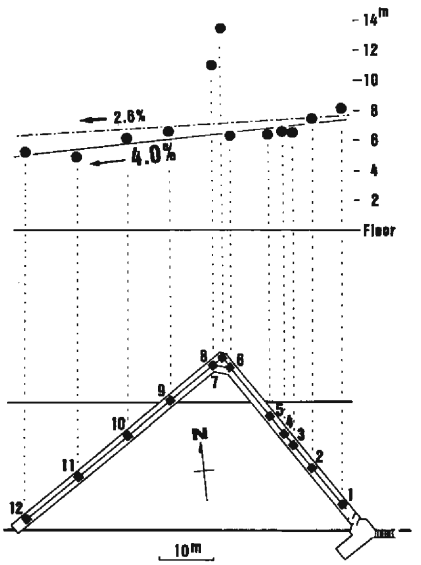


Fig. 8. Overburden depths at each sensor point obtained by calculating equation (6). The chain and solid lines show the real road surface and calculated one, respectively.

After shifting the air temperature by the phase delays given in **Table 2,** we obtained regression coefficients of thermal strain versus air temperature and subtracted the thermal strains from the observed strain variations. The results are shown in **Figs. 9a** and **b.**

### 3. 3 Secular strain variations

(1) Creep movements of the Yasutomi fault

As shown in **Figs. 9a** and **b,** long-term variations with time intervals of a few years predominate in all strain components. Nevertheless, since the investigation of creep movements is an important subject, we will discuss whether any monotonous shear movement of the Yasutomi fault is recognized throughout our twelve year observations or not. Alternate directions of secular treds were recognized between two neighboring components. This alternation was remarkable for partial strain variations in A-tunnel as shown in **Fig. 9b.** If we assume these monotonous trends of the partial strain variations as real creep movements, the strain rate reaches about $10^{-5}$ strain/year. This value is too large to be considered a deformation in the perfect elastic medium. Consequently, there might be some highly fractured portions in the basement rock in A-tunnel and the behavior of those portions is non-elastic for long-term variations. If the extensometer rod is long enough, such alternate directions of amall-scale movements are averaged, and any monotonous trend will not be detected.

As for B-tunnel, the averaged rate of secular trends of partial strains is about $10^{-6}$ strain/year and is smaller than that of A-tunnel. In other words, it is considered that highly fractured portions such as in A-tunnel do not exist in B-tunnel. The component 11-10, which crosses a thin fractured zone, showed slight extension while other

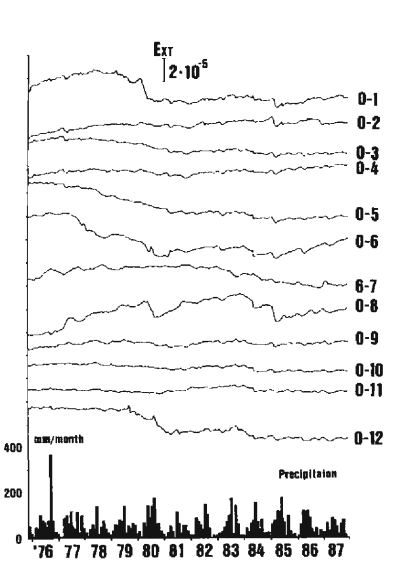


Fig. 9a

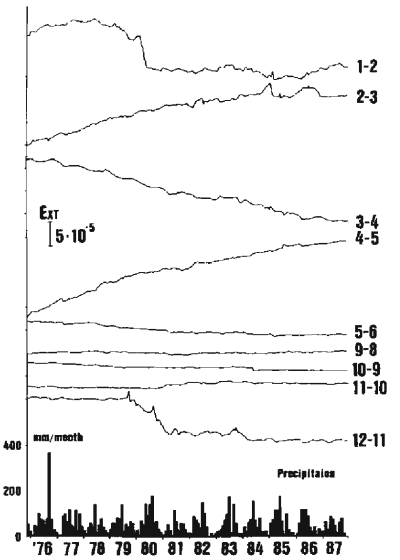


Fig. 9b

Fig. 9a. Variation of fixed-end strains and monthly precitation at the Yamasaki Fault Observation Station. The effects of the annual variation of surface temperature were already reduced.

Fig. 9b. Variation of partial strain in which annual variations were reduced.

components generally showed slight contraction.

Both A- and B-tunnels are perpendicular to each other and cross the fractured zone of the Yasutomi fault at an angle of about 45 degrees. If it is assumed from the fault topography that the left-lateral slip rate of the Yasutomi fault is 0.3mm/year[10] and the slip is borne by the whole Yasutomi fault zone of 100 meters thick, then extensional strain of $2\times10^{-5}$ should be observed in A-tunnel for these twelve years and the same amount of contraction should be observed in B-tunnel. This strain change of $2\times10^{-5}$ is of course large enough to be observed with the present extensometer system, but no such systematic strain variations are recognized. Therefore, it can be concluded that no significant left-lateral creep movement of the Yasutomi fault zone occurred during the observation period.

(2) Long-term strain variations

As shown in **Figs. 9a** and **b,** long-term strain variations with time intervals of a few years are recognized similarly in almost all strain components, except component 6-7. The strain components show common patterns including coincident turning points and identical polarities both in A- and B-tunnels. In order to show this more clearly, we have calculated low pass filtered[31] fixed-end strains with a cut-off period of 60 days (**Fig. 10**). In the figure, the averaged long-term tendency of each portion is indicated by guide lines. As seen in **Fig. 10,** both A- and B-extensometers showed extension at the first

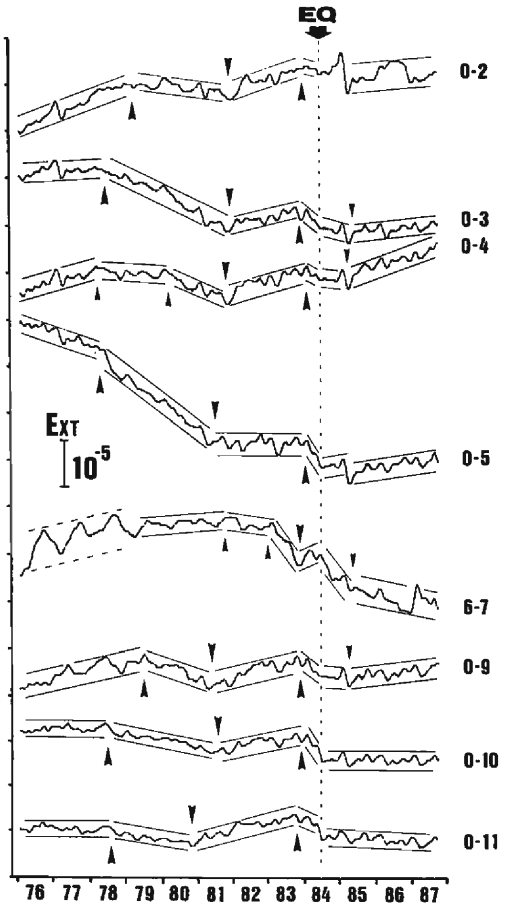


Fig. 10. Strain variations obtained by applying a low pass filter with cut-off period of 60 days. In order to emphasize the long term variations, guide lines are drawn and turning points are indicated by arrow heads.

stage and reached peaks in 1978 or in 1979. After that, the extension rate decreased and gradual contraction started. Troughs appeared from the end of 1980 to the end of 1981. After that, both A– and B–extensometers indicated extension again and reached their peaks at the end of 1983. Subsequently, all components once again contracted and the Yamasaki fault earthquake of M5.6 occurred on May 30th, 1984, which was the biggest earthquake on the Yamasaki fault throughout our twelve year observation period. After this earthquake, a turning point was recognized at the beginning of 1985, when characteristic strain variations were observed commonly in all components; short–term strain variations with time intervals of about seven to eight months were recognized before and after the Yamasaki fault earthquake. Being compared with long–term strain variations which are predominant throughout the twelve years of observation, the short–term strain variations are considered to be related to the Yamasaki fault earthquake. After this

turning point, most components in A– and B–tunnels showed slight extension in general, while the components 6–7 and 0–11 showed contraction. As described above, all strain components except component 6–7 have shown extension and contraction alternately with a periods of a few years. In this article, we tentatively call these alternate strain variations "long–term strain variations".

These long–term strain variations can also be recognized in the partial strain variations in A–tunnel. Almost components except 0–8 and 0–12 in B–tunnel also show such long–term variations. The monotonous trends are, however, so large in partial strains as mentioned in **3. 3** (1) that we cannot discuss the long–term variations of partial strains. Judging from the fact that the strain variation pattern of the two mutually perpendicular tunnels are similar in the appearance of their turning points and directions, the deformation should be either uniform or perpendicular to the fault. A shear movement cannot induce such similarity in variations as those above.

In order to decide whether the deformation is uniform or perpendicular to the fault, it is necessary to analyze the third direction of strain, component 6–7, which is situated in the direction N72°W at the corner of the vault. This component also showed extension in general till 1975. There was, however, some lack of data in this component and the reliability was low in this period. From 1978 to 1981, this component showed extension against the contraction of both A– and B–tunnels. From 1981 to the end of 1983, both A– and B–extensometers once more indicated extension, whlie component 6–7 tended to contract. In the half year period from the end of 1983 to May 1984, component 6–7 showed extension while both A– and B–extensometers showed contraction. By comparing these strain variations of three directions, it can be said that the third component of 6–7 showed the opposite direction of strain variations to those of A– and B–tunnels at least since 1978. This means that the deformation is not uniform but perpendicular to the fault zone, at least since 1978. In other words, the thickness of the fault increases when both A– and B–extensometers show extension, and decreases when A– and B–extensometers show contraction. The amplitudes of this strain variations of the thickness of the fault zone are $5\times10^{-6}$ strain. After the Yamasaki fault earthquake of May 1984, a turning point was recognized at the beginning of 1985. After this turning point, the thickness of the fault seemed to stabilize.

(3) Strain variations in the direction normal to the fault strike derived from the principal strain analyses

In order to discuss time variations of horizontal strain through principal strain analyses, strain variations of each component shown in **Fig. 9a** are divided for every half year period (December–May ; June–November). Strain changes for each semiannual interval are obtained by the least square method, by assuming that strain variations are monotonous in each of half year intervals. Principal strain axes are calculated semiannually by using the semiannual strain changes obtained.

Among many combinations of strain components, we calculated strains from the following two combinations of three directions, namely, 0–3, 0–10 and 6–7, and 0–2, 0–11 and 6–7. The former combination (0–3, 0–10, 6–7) is located on the northern side of

the main fractured zone in the vault. We call this "N–combination". The latter combination (0–2, 0–11, 6–7) crosses the main fractured zone in the vault. We call this "F–combination" in the following. The strike of the Yasutomi fault is about N100°E near the observation vault.

Variations of principal strain axis for every half year period and frequency distribution of its azimuth are shown in **Figs. 11a** and **b.** As the component 6–7 was not in good condition in the early stage, we will discuss the strain variations observed after December 1978. According to **Fig. 11a,** the directions of the principal strains of each stage derived from N–combination were comparatively coherent and changed systematically. From December 1978 to November 1981, the contraction normal to the fault zone predominated. From December 1981 to November 1983, the strain pattern was reversed and the extension normal to the fault zone predominated.

On the other hand, the directions of the principal strain axes derived from F–combination were distributed to some extent. The extension in the direction normal to the fault, however, was confirmed from December 1981 to November 1983 as shown in **Fig. 11b.** Namely, the extension normal to the fault and contraction parallel to the fault became dominant in both combinations from December 1981 to November 1983.

From December 1983, both combinations rotated their principal strain axes by 90 degrees, and the contraction perpendicular to the fault became dominant. It is supposed that at this stage a contraction occurred in the Yasutomi fault zone. After this, the Yamasaki fault earthquake of M5.6 occurred at the Kuresaka–toge fault in May 1984.[32]

A remarkable expansion normal to the fault zone was recognized during the half year after the Yamasaki fault earthquke. Since then, both combinations have shown alternate patterns with moderate amplitudes. However, the directions of principal strain have remained almost normal to the Yasutomi fault.

From these results, it can be concluded that the principal strain analyses also showed the same pattern of strain variation normal to the fault strike of the Yasutomi fault zone, as described in **3. 3** (2). Moreover, the frequency distribution of directions of principal strain axes tends to concentrate in two directions, parallel and perpendicular to the fault. The above strain variation pattern is shown schematically in **Fig. 12.**

Tabei et al. (1985)[33] reported that at Ikuno Observation Station, thirty kilometers NE from the Yasutomi Observation Vault, the similar changes as those of our results were recognized both in 1978–1980 and in 1981–1982. The turning points in their case almost coincide with those observed at Yasutomi. Furthermore, the tidal records at Kobe also showed similar turning points.[34] Therefore, such characteristic long–term variations as mentioned above might be a common phenomenon, observable over a fairly wide area. There is a suggestion that these long–term variations recognized over wide areas are related to long–term variations in precipitation.[35] Concerning our twelve year observations, however, we can not find any certain relation between long–term strain variation and precipitation.

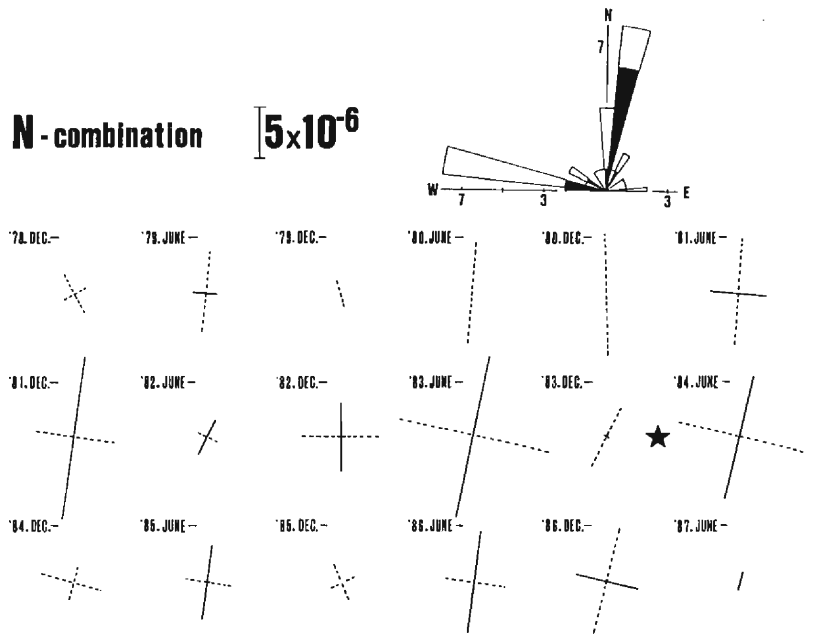


Fig. 11a. Distribution of the semiannual principal strain axes obtained by N–combination. Solid lines denote extension and broken lines, contraction. An asterisk means the occurrence of the Yamasaki fault earthquake on May 30th, 1984. Rose diagrams show the frequency distribution of azimuths of the principal axes. Black area and white area show extension and contraction, respectively.

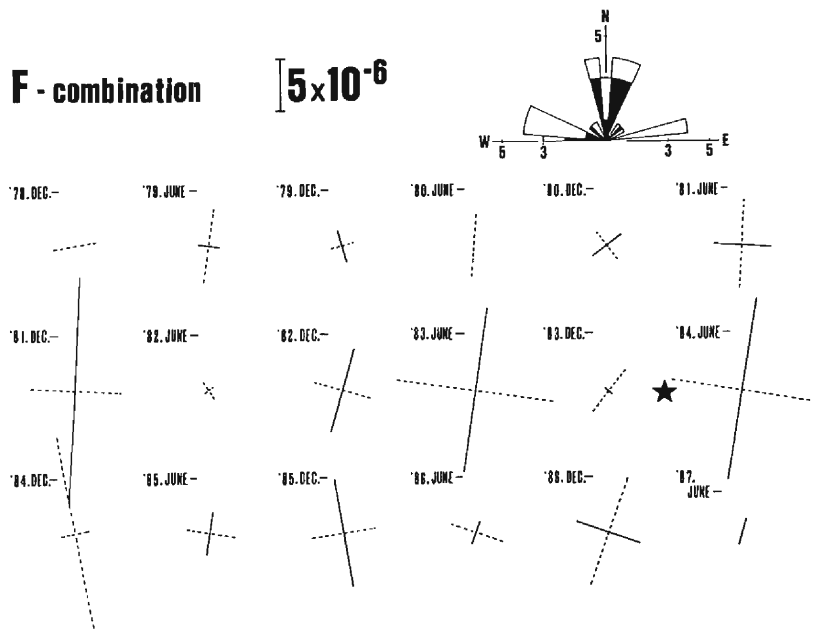


Fig. 11b. Distribution of the semiannual pricipal strain axes obtained by F–combination. Descriptions are the same as in **Fig. 11a.**

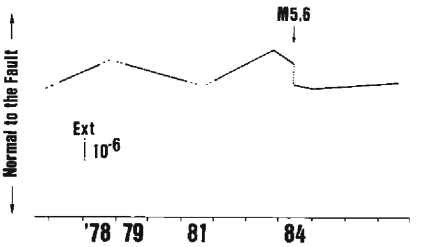


Fig. 12. Schematic diagram of the strain variations in the direction normal to the Yasutomi fault zone. The vertical axis denotes the strain change normal to the fault zone. The strain step observed at the Yamasaki fault earthquake is also drawn.

## 4. Discussion

### 4. 1 Seismic activity and the strain variation of the Yasutomi fault zone

We will compare the seismic activity around the Yamasaki fault region with the strain variation ascertained in the previous section. In this section, we utilize the accumulated number of earthquakes to represent seismic activity.

**Figs. 13a** and **b** show the epicentral distribution of $M \geqq 2$ earthquakes around the Yamasaki fault obtained by the Tottori Microearthquake Observatory network,[36] the accumulated number and their time series.[17] As shown in **Fig. 13b,** the seismic activity near the Yamasaki fault was high in the period from the middle of 1977 to the end of 1978. The seismic activity decreased after this period and the Yasutomi fault zone showed a maximum expansion normal to the fault zone from 1978 to 1979, which corresponds to the first turning point in **Fig. 12.** Seismic activity recurred from the end of 1979 to 1980. After this activity, the fault showed a trough of contraction in 1981, corresponding to the second turning point. In 1982, the seismicity returned to its ordinary level and continued till the end of 1983. Thereafter, the fault showed a peak of

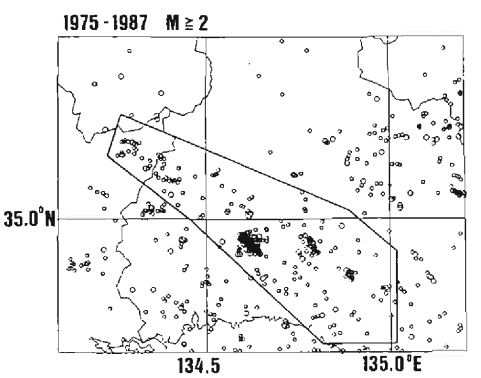


Fig. 13a. Epicentral distribution of earthquakes of $M \geqq 2.0$ and $H \leqq 40$km obtained by the Tottori Microearthquake Observatory network. The seismic activities of the surrounding area is discussed, in which the Yamasaki fault is wholly included.

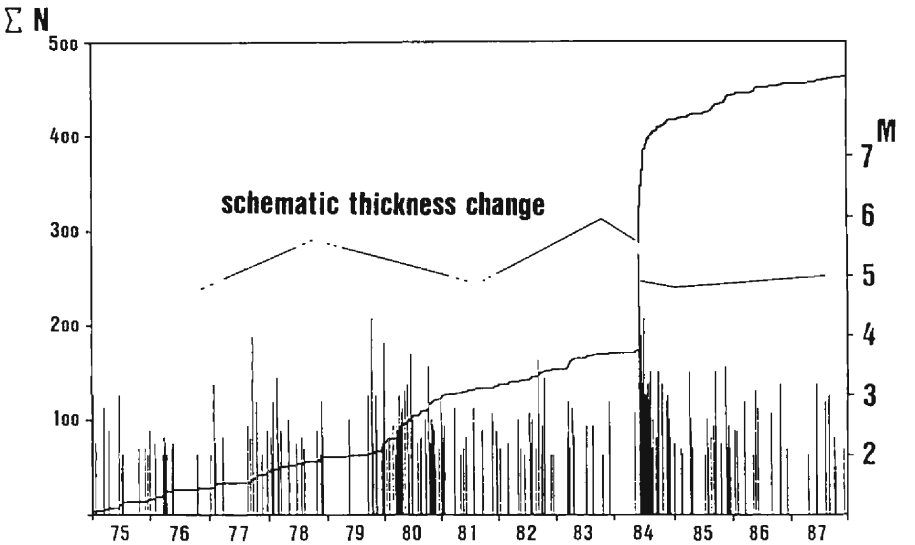


Fig. 13b. Time series of earthquakes and their accumulated number in the surrounding area. The schematic diagram of the Yasutomi fault shown in **Fig. 12** is also drawn in the figure.

expansion at the end of 1983, which corresponds to the third turning point. Throughout the seven months from November 1983 to May 1984, the seismic activity almost ceased and the Yasutomi fault showed remarkable contraction normal to the fault in this period. Subsequently, the Yamasaki fault earthquake of M5.6 occurred on May 30th, 1984.[37] Therefore, these alternate seismic activities seem to be related to the strain variations normal to the fault strike. It can thus be said that the strain variations in the Yasutomi Observation Vault also reflect the tectonic stress conditions around the Yamasaki fault.

#### 4. 2 Geodetic measurements and the strain variation of the Yasutomi fault zone

The results of geodetic measurement which have been carried out by Omura et al.[38] on the Yasutomi–Usuzuku Baseline Network are shown in **Fig. 14.** The span of the network is a few hundreds of meters and the Yasutomi Observation Vault is located inside the network. The survey has been carried out every year in November. As seen in **Fig. 14,** extension in the NS direction was large from 1975 to 1978, while contraction was large from 1978 to 1981. These variations agree well with the strain variations observed in the Yasutomi Observation Vault. Although the extensometers in the vault showed the increase of thickness of the Yasutomi fault in the period from 1981 to 1983, the geodetic measurements did not show such variations. Since this geodetic network is about ten times larger than the Yasutomi Observation Vault, this geodetic measurement may be related to wider tectonic structures outside the Yasutomi fault zone. This means that the strain variations observed by extensometers basically reflect the small-scale structure of the basement.

The Geographical Survey Institute (1987)[39] has reported horizontal strain variations

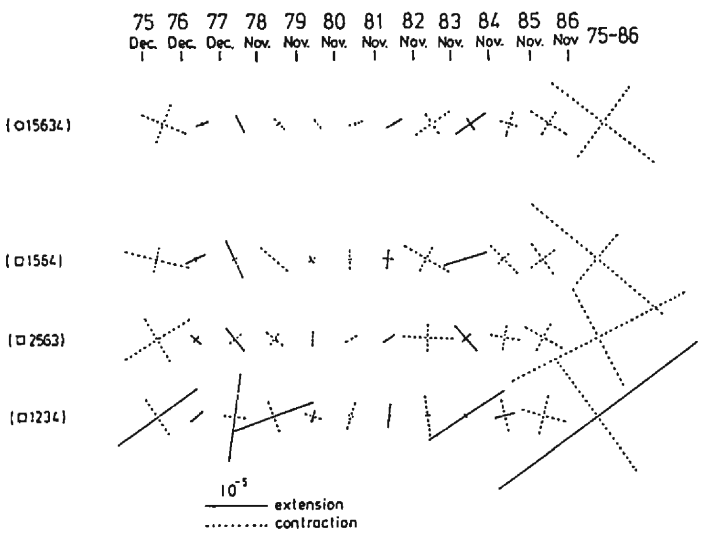


Fig. 14. Strain variations obtained by geodetic measurements. (After Omura et al.; 1988)[38]

for some tens of years including the Yamasaki fault region. According to the results, the directions of contraction range widely from NE–SW to E–W around the Yamasaki fault. This agrees with the E–W pressure axis derived from the fault plane solutions of earthquakes in this area.[40),41)] The horizontal strain over a wide area reflects the tectonic stress conditions in that area, so that the results show averaged situations, whereas the strain variations observed in the Yasutomi Observation Vault strongly depend on the structure of the Yasutomi fault. Namely, the strain field near the fault is particular and different from that of the wider area.

## 5. Conclusions

The characteristics of the Yasutomi fault zone and the fractured zones were investigated by the analyses of the extensometer records obtained at the Yasutomi Observation Vault. The results are as follows:

(1) The strain variations observed in the Yasutomi Observation Vault consist mainly of the daily variations, the annual variations, the secular variations and some other fluctuations.

(2) The daily strain variations are originated by the daily variations of surface temperature and explainable by a thermoelastic mechanism model. The amplitudes of daily strain variations range from $2\times10^{-8}$ to $5\times10^{-7}$ in summer and from $1\times10^{-8}$ to $5\times10^{-8}$ in winter.

(3) The annual variations of strain are originated by the annual variation of surface temperature, and are explained by a heat conductivity model. The amplitudes of annual strain variations range from $2\times10^{-6}$ to $7\times10^{-6}$.

(4) The long-term strain variations with time intevals of a few years were recognized

by the extensometers in three directions. The directions of these long-term strain variations were almost normal to the Yasutomi fault strike and the amplitudes of them were approximately $5\times10^{-6}$ strain. The pattern of these strain variations are interpreted as time variation of the thickness of the Yasutomi fault.

(5) The strain variations in the Yasutomi fault correlate with the seismic activity around the Yamasaki fault. This means that the strain variations at the Yasutomi Observation Vault also reflect the tectonic stress conditions around the Yamasaki fault.

(6) Before and after the Yamasaki fault earthquake, short-term strain changes with seven to eight month periods were recognized. Seismic quiescence around the Yamasaki fault was also recognized corresponding to the strain changes before this earthquake.

(7) Any systematic left-lateral creep movements of the Yasutomi fault could not be observed at least for the twelve years of the present analysis. Considering the strain rates, the amplitudes of long-term strain variations and periodic seismic activities around the Yamasaki fault, we should continue the same observations for much longer terms.

## Acknowledgments

The author would like to thank Y. Kishimoto for encouragement throughout the study and critical reading of the manuscript. Thanks are also due to K. Oike, T. Tanaka and N. Sumitomo for their valuable discussions, encouragement and critical reading of manuscript. F. Takeuchi, K. Matsumura, S. Matsuo and T. Ohkura also advised in observations and computations. K. Nakamura, the Tottori Microearthquake Observatory of Kyoto University, Japan High Way Corporation and Yasutomi Town kindly allowed us to quote valuable data and provided observation facilities. The author expresses his sincere thanks to each of them.

## References

1) Hahizume, M.: Investigation of Microearthquakes —On Earthquake Occurrence in the Crust —, Bull., Disas. Prev. Res. Inst., Kyoto Univ., Vol. 20, 1970, pp. 65-94.

2) Kishimoto, Y. and R. Nishida: Mechanism of Microeathquakes and Their Relation to Geological Structures, Bull., Disas. Prev. Res. Inst., Kyoto Univ., Vol. 23, 1973, pp. 1-25.

3) Huzita, K.: Tectonic Development of Southwest Japan in the Quaternary Period, Jour. Geoscience, Osaka City Univ., Vol. 12, Art. 5, 1969, pp. 53-70.

4) Huzita, K., Y. Kishimoto and K. Shiono: Neotectonics and Seismicity in the Kinki Area, Southwest Japan, Jour. Geoscience, Osaka City Univ., Vol. 16, Art. 5, 1973, pp. 93-124.

5) Oike, K and Y. Kishimoto: The Yamasaki Fault as a Test Field for the Earthquake Prediction, Proceedings of Earthquake Prediction Research Symposium (December 13, 14, 15th, 1976), pp. 83-90, 1977 (in Japanese).

6) Kishimoto, Y.: Test-Field Experiments for Earthquake Prediction at the Yamasaki Fault, Proceedings for Earthquake Prediction Research Symposium (1980), pp. 133-142, 1980 (in Japanese).

7) Kishimoto, Y.: On Precursory Phenomena Observed at the Yamasaki fault, Southwest Japan, as a Test-Field for Earthquake Prediction, Earthquake Prediction; An International

Review, Maurice Ewing Series 4, 1981, pp. 510–516.
8) Oike, K. and K. Nakamura: Results of Continuous Observation by Extensometers at the Yamasaki Fault, Annuals, Disas. Prev. Res. Inst., Kyoto Univ., No. 21B–1, 1977, pp. 11–18 (in Japanese).
9) Watanabe, K., K. Oike, K. Nakamura and Y. Kishimoto: On the Characteristics of Long-Period Strain Change in the Yasutomi Observation Tunnel at the Yamasaki Fault, Annuals, Disas. Prev. Res. Inst., Kyoto Univ., No. 26B–1, 1983, pp. 87–94 (in Japanese).
10) The Research Group for Active Faults: Active Faults in Japan, University of Tokyo Press, 1980.
11) Ando, K.: Miura-hanto, Izu-hanto oyobi Hyogoken Yamasaki fukin ni okeru dansou no yokozure ni yoru tani no hen'iryo ni tsuite, Geographycal Review of Japan, 45–10, 1972, pp. 716–725 (in Japanese).
12) Huzita, K.: Yamasaki Fault System, Proceedings for Earthquake Prediction Research Symposium (1980), pp. 143–147, 1980 (in Japanese).
13) Fukui, K.: Fault Topography along the Yamasaki Fault System, Western Kinki District, Japan, Geographycal Review of Japan, 54–4, 1981, pp. 196–213 (in Japanese).
14) Geological Survey of Japan: 1/200,000 Geological Map (Himeji), 1981.
15) Oyo corporation: Report on the Yasutomi boring, 1988 (in Japanese).
16) Okada, A., M. Ando and T. Tsukuda: Trenching Study for Yasutomi Fault of the Yamasaki Fault System at Anji, Yasutomi Town, Hyogo Pref., Japan, —Chigaku Zasshi—, Vol. 96, No. 2 (887), pp. 81–97 (in Japanese).
17) Ishikawa, Y., K. Matsumura, H. Yokoyama and H. Matsumoto: SEIS-PC—its outline—, Joho Chisitsu, Vol. 10, pp. 19–34, 1985 (in Japanese).
18) Japan High Way Corporation: Personal Communcation.
19) Oike, K.: Personal Communication.
20) Oike, K., K. Watanabe, K. Nakamura, K. Taniguchi and Y. Kishimoto: On the System for the Continuous Observation in a Test-Field for the Earthquake Prediction at the Yamasaki Fault, Annuals, Disas. Prev. Res. Inst., Kyoto Univ., Vol. 24B–1, pp. 29–40, 1981 (in Japanese).
21) The Geodetic Society of Japan: General View of Geodesy, 1974, pp. 209–214 (in Japanese).
22) Nakano, S.: The Effect of Surface Temperature on the Crustal Deformations, Bull., Disas. Prev. Res. Inst., Kyoto Univ., No. 60, 1963, pp. 2–20.
23) Yoshioka, H. and S. Nakano: Strains in a Semi-Infinite Elastic Solid Caused by Temperature Variation on Its Free Surface, Jour. Seis. Soc. Japan, Vol. 27, No. 1, 1974, pp. 25–41 (in Japanese).
24) Tanaka, T.: Study on Meteorological and Tidal Influences upon Ground Deformations, Special Contr. Geophys. Inst., Kyoto Univ., No. 9, 1969, pp. 29–90.
25) Tanaka, Y.: Chikakuhendou no Nenhenka to kansokuten no Fukasa, Program and Abstracts, The Geodetic Society of Japan, 1972, pp. 18–19 (in Japanese).
26) Himeji Meteorological Station: Monthly Report (in Japanese).
27) Berger, J.: A Note on Thermoelastic Strains and Tilts, Jour. Geophys. Res., Vol. 80, No. 2, 1975, pp. 274–277.
28) Ben-Zion, Y. and P. Leary: Thermoelastic Strain in a Half-Space Covered by Unconsolidated Material, Bull. Seis. Soc. America, Vol. 76, No. 5, 1986, pp. 1447–1460.
29) Watanabe, K.: An interpretation of the annual ground strain variation using one-dimensional thermal conductivity model, Earth Science Report of College of Liberal Arts and Science, Kyoto Univ., Vol. 22, pp. 13–21 (in Japanese).
30) Tokyo Astronomical Observatory(ed): Rika nenpyo (Chronological Scientific Tables), Maruzen Co. Ltd., Vol. 60, 1987.
31) Saito, M.: An Automatic Design Algorithm for Band Selective Recursive Digital Filters, Physical Exploration (Butsuri Tanko), Vol. 31, No. 4, 1978 (in Japanese).
32) The Research Group for the Yamasaki Fault: Research Papers on the Yamasaki fault, Part 1 and 2, 1988.
33) Tabei, T., K. Fujimori and Y. Tanaka: Observations of Crustal Movements at Ikuno (1977–1983), Jour. Geodetic Soc. Japan, Vol. 31, No. 2, pp. 189–201, 1985 (in Japanese).

34) Earthquake Research Institute, The University of Tokyo: Vertical Crustal Movements in Japan as Deduced from Tidal Records (1951–1987). Report of the Coordinating Committee for earthquake Prediction, Vol. 41, pp. 498–520, 1989 (in Japanese).
35) For example, Shichi, R: Personal Communication.
36) Tottori Microearthquake Observatory: Personal communication.
37) Shibutani, T. and K. Oike: On Features of Spatial and Temporal Variation of Seismicity Before and After Moderate Earthquakes, Jour. Phys. Earth, Vol. 37, pp. 210–224, 1989.
38) Omura, M., K. Fujimori, S. Otsuka, K. Nakamura and Y. Tanaka: Geodetic Monitoring of the Crustal Movements across the Yamasaki Fault, Southwest Japan, Bull., Disas. Prev. Res. Inst., Kyoto Univ., Vol. 38, pp. 79–97, 1988.
39) Geographical Survey Institute: Horizontal Strain in Japan, 1987.
40) Kishimoto, Y. and R. Nishida: Mechanism of Microeathquakes and Their Relation to Geological Structures, Bull., Disas. Prev. Res. Inst., Kyoto Univ. Vol. 23, part 1, No. 210, pp. 1–25, 1973.
41) Ohkura, T: Focal Mechanisms of Shallow Earthquakes which Occurred in San'in, Kinki and Hokuriku Districts, Jour. Seis. Soc. Japan, Vol. 41, pp. 89–96, 1988 (in Japanese).